ELSEVIER

International Journal of Mass Spectrometry 215 (2002) 31–43

International Journal of Mass Spectrometry

www.elsevier.com/locate/ijms

Evaluation of a microsphere plate detector for an orthogonal acceleration matrix-assisted laser desorption/ionisation time-of-flight mass spectrometer

D.S. Selby, V. Mlynski, M. Guilhaus*

School of Chemistry, The University of New South Wales, Sydney 2052 Australia

Received 7 September 2001; accepted 7 November 2001

Abstract

A single 70 mm diameter microsphere plate (MSP) detector was evaluated in an orthogonal acceleration time-of-flight mass spectrometer fitted with a matrix-assisted laser desorption/ionisation source. The ion energy of the spectrometer was approximately 20 kV. The results indicated that the detector performance was excellent, for a single plate device, in terms of background count-rate, temporal characteristics of the pulses and the gains for single ions. A background count rate was observed to be less than 1 count s^{-1} cm^{-2} and the single-ion pulse width was about 800 ps at half height. The plate displayed a gain in the range 1×10^6 to 3×10^6 for all masses tested. The single ion gain measurements showed no significant decrease with mass while the summed signal intensity (total observed counts) decreased strongly at high mass. The gain distribution data were interpreted in conjunction with this observation to indicate that the detector efficiency was poor for high mass ions. (Int J Mass Spectrom 215 (2002) 31–43) © 2002 Elsevier Science B.V. All rights reserved.

Keywords: Time-of-flight; MALDI; Orthogonal acceleration; Detector

1. Introduction

All mass spectrometers require some form of ion detector. A detector suitable for time-of-flight mass spectrometry (TOFMS) should have a rapid response time, a high gain and good conversion efficiency. These specifications allow the detection of (preferably) single ions with excellent time resolution. Ideally, the detector should have a time resolution much better than the analyser, so it will have a negligible effect on the instrument's final resolution [1]. A matrix-assisted laser desorption/ionization (MALDI) ion source has the ability to generate singly-charged ions of over 1×10^6 Da [2], so it is also desirable for the detector to give good responses at high mass. Additionally, quantitative analytical work requires response to be proportional to the amount present.

It is difficult to find a detection system that adequately fulfils all the above criteria. Most current MALDI-TOFMS instruments utilise microchannel plate (MCP) detectors, with (usually) an integrating transient recorder monitoring the output [3]. MCP detectors are flat, provide time resolution of the order of a nanosecond and provide high gain at low mass.

While an MCP provides a good compromise for conventional MALDI-TOF instruments, use of an orthogonal acceleration (oa)-TOF analyser adds a further requirement. An oa-TOF analyser works best

* Corresponding author. E-mail: m.guilhaus@unsw.edu.au

PII S1387-3806(01)00565-6

with ions of constant desorption energy, regardless of mass, whereas MALDI produces packets of ions with increasing energy as mass increases [4]. This spread in desorption energy, if uncorrected, requires a long orthogonal accelerator (in the desorption axis) to allow most of the ions to enter the field-free flight region. The spatial distribution of ions is increased even further by the time ions reach the detector plane. Detection of most of these ions requires a large detector, when compared to other TOF instruments. It is desirable to detect most of these ions, to provide high sensitivity and optimal signal-to-noise ratio.

Large MCPs are expensive, so a detection system was developed here incorporating a microsphere plate (MSP), a newer and less expensive alternative. Use of an MSP had not been reported in a TOF mass spectrometer, although a patent has been granted in which a linear TOF instrument is combined with an MSP detector [5]. Since the detector was relatively novel, it has been evaluated to determine how well it satisfied the necessary criteria.

1.1. Principles of the microsphere plate detector

An MSP is formed by sintering glass beads of 20–100 μm diameter into a glass plate (0.7 mm thick for a single thickness plate, such as the one used in this study). This creates a thin plate with irregularly shaped channels between the planar faces. The surfaces of the beads are covered with an electron emissive material and the faces of the plate are coated to make them conductive. When an appropriate potential is applied across the plate, it acts as an electron multiplier, functioning in a similar manner to an MCP. An outline of its operating principles is discussed below. More detailed principles are given in papers by Tremsin and co-workers [6,7] and Naaman and Vager [8].

An operational MSP is placed inside a vacuum chamber and a potential difference of between 1.5 and 3.5 kV is applied across the plate, with the back face of the MSP at the more positive potential. When a fast moving particle or a photon is incident on the front of the detector, it causes the emission of an integral number of '*initial secondary electrons*'. The electric field ensures these electrons are accelerated into the channels of the detector. When one of these electrons hits the surface of a bead inside the channel, it causes the emission of a number of secondary electrons, provided the electric field has accelerated it sufficiently. Each of the secondary electrons is itself accelerated and causes the release of a number of secondary electrons when it collides with the walls. This process is repeated a number of times, as illustrated in Fig. 1, significantly amplifying the signal. When monitored with an integrating transient recorder, the output of the MSP is recorded as a pulse.

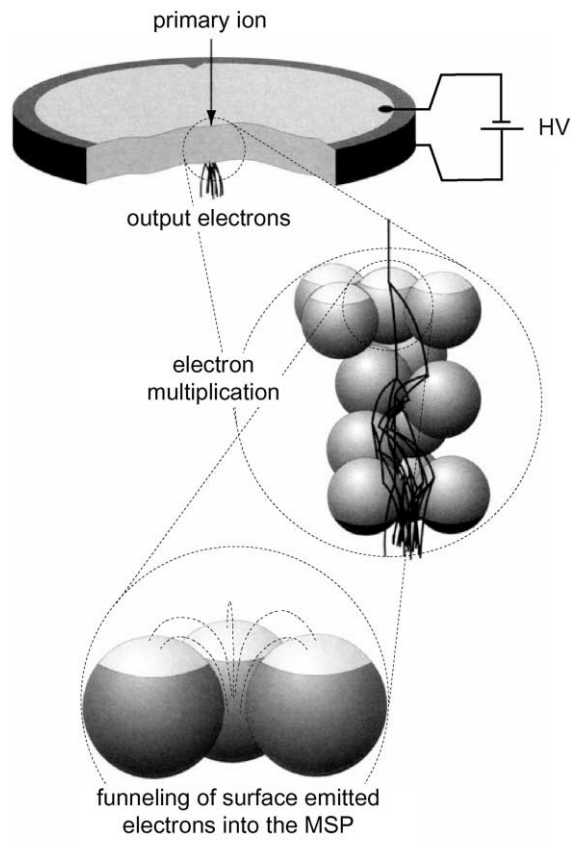

Fig. 1. Diagram of an MSP, illustrating the sintered glass construction and secondary electron multiplication cascade.

Earlier investigations of MSP behaviour utilised UV photons [6,7]. Performance as an ion detector was unlikely to be identical. For instance, the performance of electron multipliers varies with the *m*/*z* of the ions, and it is known that they operate less efficiently with higher mass ions [9,10]. Thus, the detection system of the mass spectrometer was thoroughly evaluated, with particular attention paid to background noise, pulse width, effect of bias potential on gain, and the extent of mass discrimination in gain.

2. Experiment

2.1. Apparatus

The detector was developed for a custom built MALDI oa-TOFMS mass spectrometer that has been described in detail elsewhere [11]. The mass spectrometer has its source operating at ground potential and the drift-region floating at the accelerating potential of approx. −20 kV. Floating the drift region in this way is typical for oa-TOF instruments [4] and it usually results in the front face of the detector also being at the drift region potential. In this case, the potential is much higher than a typical multiplier bias potential. Decoupling the detector signal from the high voltage was therefore required in order to allow the transmission line and detection electronics to operate at ground potential. This was achieved by allowing the MSP's output electrons to fall through ∼17 kV, behind the MSP plate biased at ∼3 kV, before registering on the collector plate, as described below. The detection electronics consisted of a 4 GS/s LeCroy 9384 transient recorder (LeCroy Corporation, NY, USA) and, when required, a 1 GHz Ortec 9306 preamplifier (EG & G Ortec, Oak Ridge, TN, USA).

For all experiments, unless otherwise stated, the apparatus was set to its standard operating potentials of −20 kV for the analyser, +1.3 kV for the mirror and +1.0 kV for the push out pulse. These potentials were applied for 1–2 hours before conducting any measurements, to allow the power supplies and detector to reach their respective operating temperatures.

2.2. Detector assembly

The heart of the detection system was a 70 mm diameter single thickness MSP electron multiplier, obtained from El-Mul (Yavne, Israel). The manufacturer's specifications are given in Table 1. The maximum potential drop allowed across the detector was 3.5 kV, while the baseline potential required for the oscilloscope used to monitor the detector's output was ground. The front of the detector had to be at the acceleration potential, −20.0 kV, with the back at approximately −17 kV. This meant that the electrons emerging from the back of the MSP could not be directly monitored by the oscilloscope, since the oscilloscope's input had to be close to ground. Thus, the detection system was designed to allow the electrons' potential to fall through a uniform field, 41 mm in length, before they reached the collector plate, with the resulting transient signal monitored by an oscilloscope. The uniform field was set up with five spacer rings and a resistor chain, as illustrated in Fig. 2. Simulations indicated that when the accelerator potential was set to −20 kV, electrons would take approximately 1.1 ns to travel from the back of the MSP to the collector plate. A negligible spread in electron transit time was apparent due to different starting positions from the back of the MSP.

Table 1
Manufacturer's specifications for the MSP used in this study

Parameter	Value
Plate diameter (mm)	70
Active input surface diameter (mm)	67
Active output surface diameter (mm)	68.6
Thickness (mm)	0.70
Sphere diameter (μm)	60
Maximum bias potential (kV)	3.0
Resistance (MΩ)	23–31
Pulse width (ns)	<1
Dark current (nA)	12

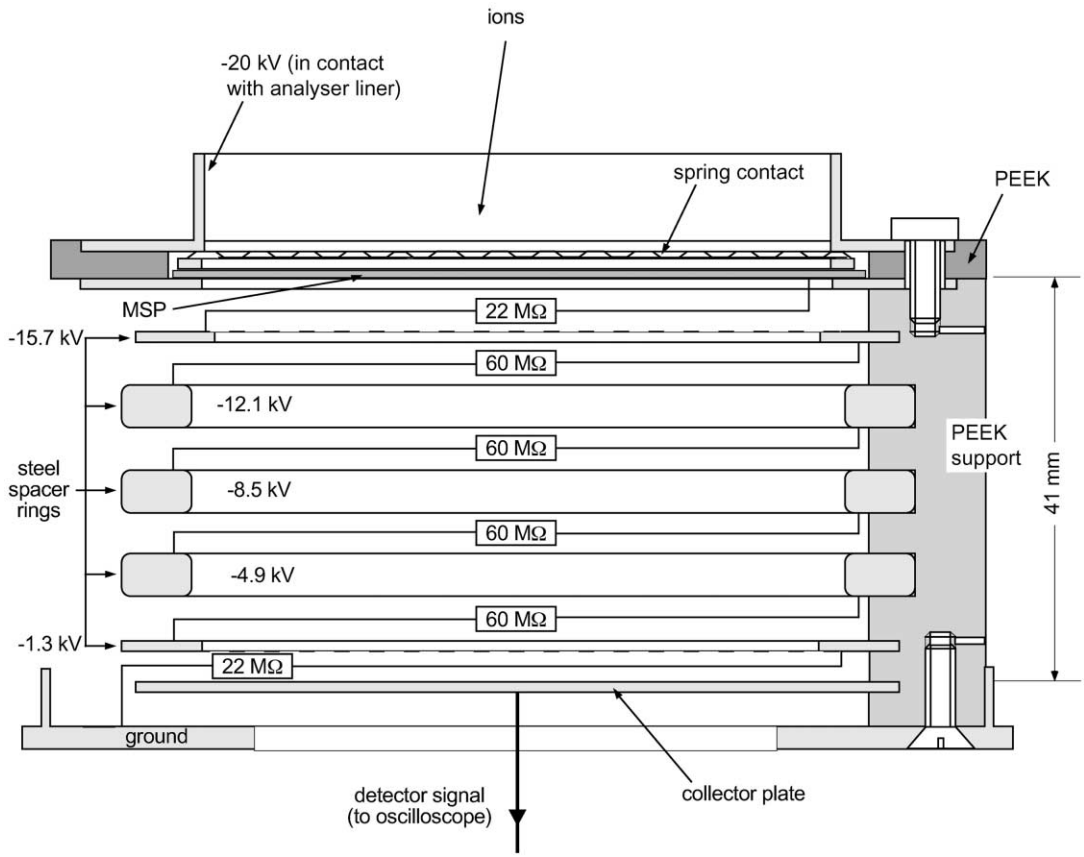

Fig. 2. Diagram of the detector assembly, with resistors and potentials listed. The 22 M resistances represent single resistors, while each 60 M resistance represents a chain of 1×15, 1×12 and 1×33 M resistor, connected in series. The front of the MSP is at -20.0 kV and the back of the MSP is assumed to be at -17.0 kV. The potentials on the spacer rings were calculated based upon the resistor chain.

The bias across the MSP was controlled with an external resistor (R), connected in parallel with the MSP, via two feed-throughs. Two settings were available for R, giving a detector bias of 2.94 kV (low gain setting) or 3.15 kV (high gain setting) when the accelerator supply was set to -20.0 kV. This resistance was kept lower than the resistance of the MSP, ensuring the potential across the MSP was set by R.

The possibility of damage from electrical discharge in the detector, e.g. from vacuum accidents, was reduced by limiting the total current from the power supply to 0.5 mA (half the specified maximum allowable current).

2.3. Sample preparation

The experiments involving single ions were performed with samples of 2,5-dihydroxybenzoic acid (DHB) matrix, bovine insulin and horse heart myoglobin, all obtained from Sigma (St. Louis, MO, USA) and used without further purification. Gramicidin S of unknown origin was also used, after it was determined to be pure by mass spectrometry. All analytes and the matrix were dissolved in 1:1 (v/v) acetonitrile and 0.5% aqueous triflouroacetic acid. Samples of gramacidin S, insulin and myoglobin were prepared by the dried droplet method with DHB matrix present in a 1000-fold molar

excess. A sample containing only DHB matrix was also prepared.

3. Results and discussion

3.1. Background count rate and dark current

Background counts and dark current signals in electron multipliers are usually due to field emission and outgassing events within the detector. The detector's background count rate and dark current were measured, since both these factors determined its background noise characteristic. It was, however, difficult to monitor the direct output of the detector, due to the small output voltages corresponding to the background signals. This was overcome by using the Ortec (100× gain) pulse amplifier to increase the potential of the output signals to a voltage that could be easily monitored, without increasing the number of counts or current. One of the output channels was connected to the LeCroy 9384 Oscilloscope, to provide direct monitoring of the output signal. The other output was connected to a Hewlett-Packard 5382A 255 MHz frequency counter, set to a 10 s gate (Hz frequency range), with a 10× attenuator. The counter's threshold for detection was 2.5 mV and with a net gain/attenuation this corresponded to a pulse amplitude of 0.25 mV. After the warm up period, the background count rate was monitored for 25 min, with the MSP set to the low gain setting. The frequency of background counts during this interval was measured with the frequency counter, giving approximately 150 readings, with the trace on the oscilloscope confirming that background counts and not electronic noise was monitored. MSP bias was adjusted to the high setting, left to warm up for 30 min, and the process was repeated.

Histograms of the count rates obtained are presented in Fig. 3, and a summary of the background count rates obtained is given in Table 2. Both the total count rate and the rate per unit area are given. The total rate is important in determining the contribution of background counts to noise in experiments on this instrument, while the rate per square centimetre allows these count rates to be compared with those obtained with other detectors. These count rates represent a worst case noise considering that the effective 0.25 mV threshold level was close to the baseline noise of the oscilloscope as it was typically used, without the preamplifier, to acquire spectra.

Dark current was monitored in a separate experiment. The instrument was set up as described above for background counts, except that a picoammeter was connected in place of the frequency counter. This allowed the background current, rather than frequency of counts, to be monitored. The device used was a Keithley 485 Autoranging picoammeter (Keithley Instruments Inc., Cleveland, OH, USA). The MSP was

Table 2
Background count rates obtained from the MSP detector with bias set to 2.94 and 3.15 kV[a]

	Bias (kV) (no. of samples)		
	2.94 (154)	3.15 (132)	2.94 and 3.15 (286)
Raw results			
Mean count rate[b] (s^{-1})	20.4	18.5	19.5
Standard deviation (s^{-1})	7.8	9.3	8.6
Range (s^{-1})	3.5–46.9	3.7–59.2	3.5–59.2
Rate per unit area[c]			
Mean count rate ($s^{-1}\,cm^{-2}$)	0.58	0.52	0.55
Standard deviation ($s^{-1}\,cm^{-2}$)	0.22	0.26	0.24
Range ($s^{-1}\,cm^{-2}$)	0.10–1.33	0.10–1.68	0.10–1.68

[a] Counter threshold was 2.5 mV.
[b] A low effective threshold of 0.25 mV was used (see text).
[c] This was found by dividing the raw results by the active input surface area of the detector (35.3 cm^2).

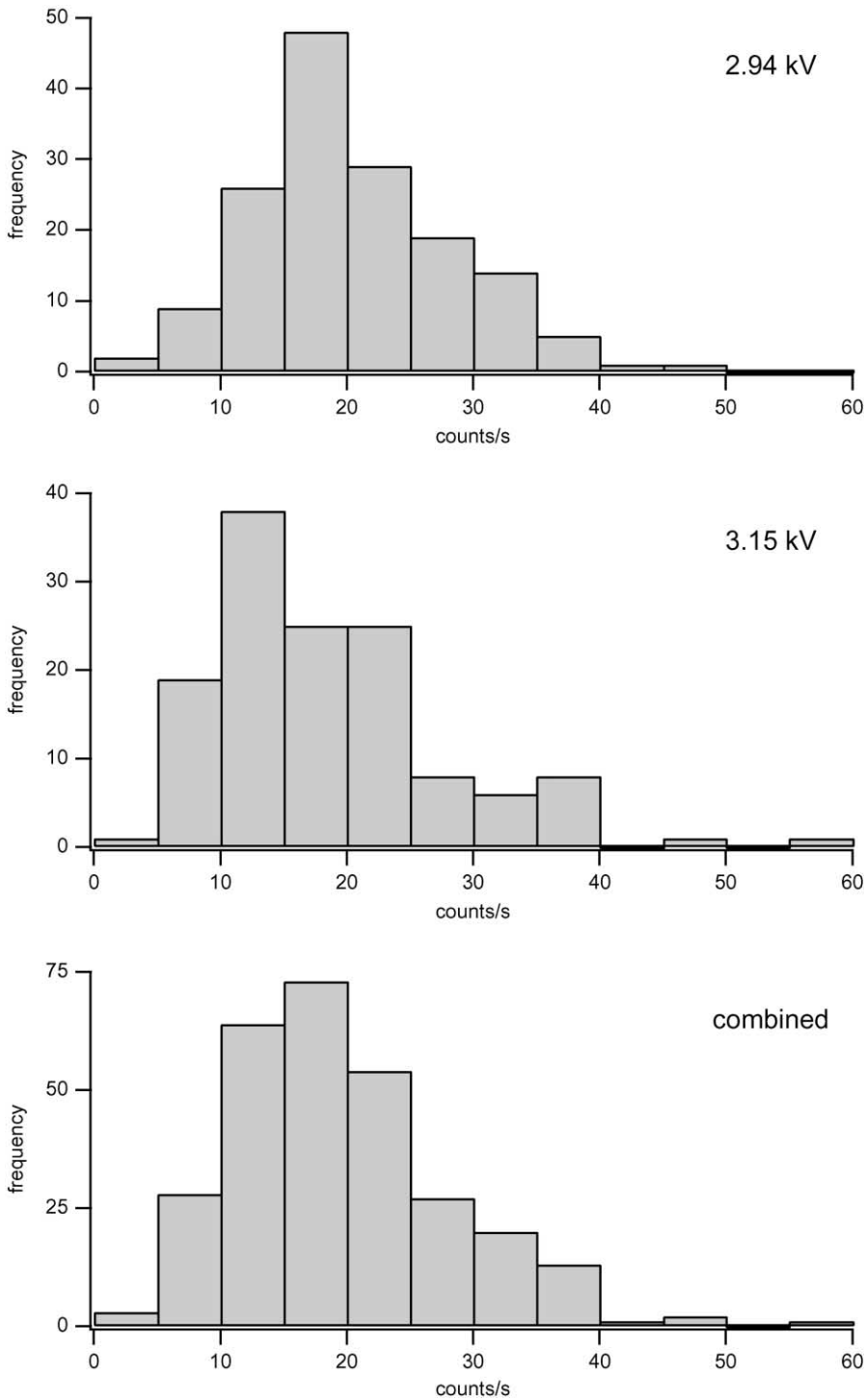

Fig. 3. Frequency histograms of background count rate, for both detector bias settings and combined results.

Table 3
Probability of zero to five background events being recorded over 100 × 100 μs sweeps

Background events	Probability (%)	
	0.1	0.3
0	90.48	74.05
1	9.057	22.28
2	0.449	3.319
3	0.015	0.326
4	0.0004	0.024
5	0.0000	0.001
Total	100.0000	99.9999

set to the low gain and the background current monitored for 25 min by inspection of the readings. MSP bias was adjusted to the high setting and the process repeated after a further stabilisation period. The dark current was observed to vary between 14.5 and 15.3 nA at both gain settings. This was only slightly above the manufacture's quoted dark current of 12 nA.

The background count, of 10–30 s^{-1} (1 standard deviation), with each signal of approximately 2 ns at the baseline, gives background interference for 10–30 discrete events over 20–60 ns in every second. If it is assumed that these events are more or less evenly distributed, it is possible to estimate the contribution of this background to spectra. Spectra recorded on this instrument spanned no more than 100 μs. Each 100 μs sweep had an (approximately) 0.1–0.3% chance of having a background peak, and a vanishingly small probability of recording more than one background peak. The probability of recording 0–5 background peaks over 100 averaged 100 μs sweeps may be calculated with the binomial distribution (Eq. (1)). The results of this are given in Table 3. It is clear from these calculations that the background from the detector has a negligible effect on the spectra recorded on this instrument.

$$p_k = \frac{n!}{k!(n-k)!} p^k (1-p)^{n-k} \quad (1)$$

Note: p_k is the probability of k events, n the number of repetitions, and p the probability for a single event.

Comparison of the dark current and the background count rate can be shown to imply a detector gain of about 5×10^9. This is unreasonably high and most probably indicates that the majority of the dark current can be attributed to events that produce pulses below the threshold of the pulse counting system.

3.2. Temporal response

The analyser power supply was turned on with detector bias set to 2.94 kV. After the warm up period the peak width (FWHM) was measured for 120 single ion peaks, obtained from a sample of DHB (*m*/*z* 130–270). The mean width was 840 ps, with a standard deviation of 130 ps. The narrowest peak was 630 ps and the widest peak was 1500 ps at half height. The majority of signals were less than 1 ns, which corresponded with the manufacturer's pulse width specification.

3.2.1. Mass dependence of gain and detector conversion efficiency

It was very important to determine the relative efficiency of the detector at different masses, since MALDI is able to generate ions with mass to charge ratios ranging over at least five orders of magnitude. Samples of DHB and the analytes gramicidin S, insulin and myoglobin in DHB matrix were used to obtain signals over the mass range 130–17,600. Detector bias was set to the low gain setting. Conditions were adjusted for each sample such that, in the appropriate mass range, only single or no ions were detected. Single ion signals were taken to be narrow peaks (no wider than 2.25 ns at half height) with a *S*/*N* of 3 or more. The settings and mass range monitored for each sample are listed in Table 4. In all, 100 single ion signals were recorded for each sample. The signal obtained in the appropriate mass range from a clean portion of the sample slide was monitored, before commencing these measurements, to ensure that there was no interfering background signal. In all instances there was no such background signal. Once this experiment was completed, the process was repeated with the detector bias set to the high gain setting.

The areas of the single ion peaks were measured, after the data had been rescaled to reflect the voltage setting of the oscilloscope. These areas were then

Table 4
Settings for each sample in mass dependence of gain experiments

Sample	*m/z* range recorded	Probe voltage (V)	Lens voltage (V)	Delay (μs)
DHB	130–270	50	0	3–5
Gramicidin S	900–1300	178–179	0	33
Insulin	5300–6100	178–179	74–76	18–19
Myoglobin	16200–17600	171	74–76	60

converted to gain measurements. Gain is determined according to Eq. (2)

$$g = \frac{q}{ne} \tag{2}$$

where g is the gain; q the charge measured by the oscilloscope; n the number of unit charges incident on the detector (1 for these experiments); and e is charge of an electron. While n and e were known, q had to be calculated from the measured signal, as follows. Current can be calculated from the definition of resistance:

$$I = \frac{V}{R}$$

Current is also the rate at which charge changes, $\mathrm{d}q/\mathrm{d}t$. Thus,

$$\frac{V}{R} = \frac{\mathrm{d}q}{\mathrm{d}t}$$

Integrating this with respect to time and making q the subject gives

$$q = \frac{1}{R}\int V(t)\,\mathrm{d}t \tag{3}$$

$\int V(t)\,\mathrm{d}t$ corresponds to the area, A, under the single ion peak. On substitution into (2) this gives

$$g = \frac{A}{Rne} \tag{4}$$

The effective impedance of the detection circuit was 25.0 Ω. Substituting in the known constant values for R, n and e gives Eq. (5)

$$g = \frac{A}{4.01 \times 10^{-18}} \tag{5}$$

The calculated gain values ranged from 0.5×10^6 to 10×10^6 for the low gain results and 0.6×10^6 to 12×10^6 for the high gain results. The means and standard deviations of the gains for each mass at each bias potential were determined. A pooled result was also calculated over all the masses at each detector bias setting. These results are presented in Table 5. The mean gain for the pooled values, 2.2×10^6 at 2.94 kV and 3.1×10^6 at 3.15 kV, are very good for a single thickness plate, although lower than the gain of 6×10^6 claimed by the manufacturer for a new plate. The mean gain increased for all mass ranges

Table 5
Mean gains at different masses and bias potentials

m/z	Detector bias			
	2.94 kV		3.15 kV	
	Mean gain/10^6	Standard deviation of gain/10^6	Mean gain/10^6	Standard deviation of gain/10^6
130–270	2.13	1.78	3.50	2.80
900–1300	2.12	1.14	2.57	1.65
5300–6100	2.19	1.38	2.88	1.96
16200–17600	2.33	1.30	3.27	2.24
Pooled	2.19	1.42	3.06	2.22

except 16,200–17,600 at the higher bias setting and the pooled mean at the lower bias setting increased by 39%. This effect is smaller than the relative standard deviation for all sets of measurements, which ranged from a low of 53% for *m*/*z* 900–1300 at a bias of 2.94 kV, to a high of 84% for *m*/*z* 130–270 at the same bias. This result was consistent with the earlier observations of background counts that showed increasing pulse amplitude with bias voltage. Surprisingly, the results did not show the expected trend with mass.

Detector sensitivity to single ions was expected to decrease with mass, in an analogous manner to other electron multipliers [9]. The experiments reported earlier [11] had shown a decrease in sensitivity at higher mass, particularly for masses of over 5000. This decrease can be attributed to (1) the geometry limitations of the instrument, which meant that not all ions at higher mass would be detected; (2) any decrease in efficiency of the detector as mass increased; and (3) increasing fragmentation of ions with mass prior to the final drift region, between the ion mirror and the detector. The analyser had been especially designed with a wide oa and large detector to minimise losses due to geometry, for known ion desorption velocity spreads. Conventional MALDI instruments are known to have lower sensitivity in reflecting mode for high mass ions, due in part to fragmentation, a feature utilised in post source decay experiments [12]. This alone could not explain our dramatic fall in sensitivity. Commercial TOF instruments incorporating ion mirrors, with similar flight times, are able to record spectra of substances such as myoglobin. Thus, ion fragmentation in the first drift region was also not the critical cause of loss of sensitivity. Hence, it was postulated that a very significant contribution to decreasing sensitivity was from the detector performance.

Detector sensitivity is likely to decrease with increasing mass, due the decreasing average number of initial secondary electrons generated when an ion collides with the detector. Therefore, the results were analysed in this context. The global mean and standard deviation of a set of gain data only provide a good measure of the detector's statistical performance when the raw data is normally distributed. The mean and standard deviation do not indicate the distribution, and it is not safe to assume that single ion pulse areas from an electron multiplier are normally distributed. As described earlier, electron multipliers work by causing increasing numbers of secondary electrons to be emitted after each collision of a secondary electron with active surface of the detector. Each subsequent collision releases an integral number of electrons and it is likely that, for each initial secondary electron, the actual signal will be normally distributed. Each ion incident on the detector can be expected to dislodge either zero or an integral number of initial secondary electrons. If no electrons are emitted the ion will not be detected. If one electron is emitted a signal will be detected. A large number of "one electron" results would be expected to provide normally distributed results around a mean. If two electrons are emitted by an ion, the detected signal would be larger. A large number of "two electron" results would be expected to be normally distributed around a mean value approximately twice that of a "one electron" result. The process is similar where there are a larger number of initial electrons. Thus, if different numbers of initial secondary electrons are emitted, the single ion data would be expected to be multimodal or have one or more high gain shoulders, and not be normally distributed around a single mean. The lowest gain value mode would be expected to indicate the "one electron result", the next the "two electron" result and so on for the higher gain modes.

In a real detector there are of course other effects, such as sensitivity variations in the inside channels of the multiplier or gain saturation near the ends of the channels, that may overwhelm the effects on gain due to initial secondary electron emission. However, it was still important to plot frequency histograms of the data, as this will show the distribution of the results. A shift in the mode or skewed distribution would be expected when gain increases slowly, due to increasing emission of subsequent secondary electrons over part or all of the detector. This may occur where gain increases arise from an increase in the detector bias. Changes in a multimodal distribution or changes in shoulders, which do not change the gain value of the primary mode would be expected for differences in

initial secondary electron emission. Such a result may be expected for a different momentum and/or structure of the impacting ion.

In these experiments, all data were binned in the same manner, to allow direct comparison of the histograms. A total of 27 bins of equal width were used, spanning the full range of gain values obtained. The resulting distribution of gains for the different masses are plotted in Fig. 4 for a detector bias of 2.94 kV and Fig. 5 for a detector bias of 3.15 kV.

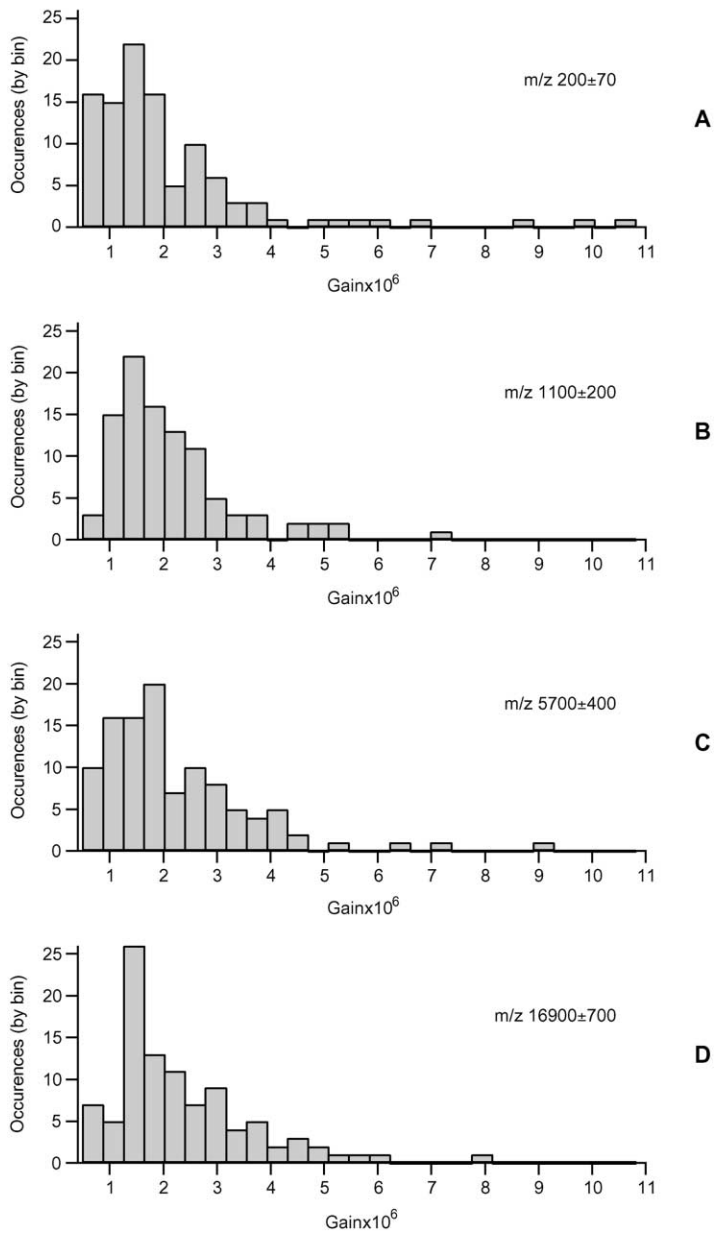

Fig. 4. Distribution of gains obtained for single ion peaks when detector bias was set to 2.94 kV. (A) Represents results for matrix ions, (B) for gramicidin S, (C) for insulin, and (D) for myoglobin, with the mass range listed on each plot.

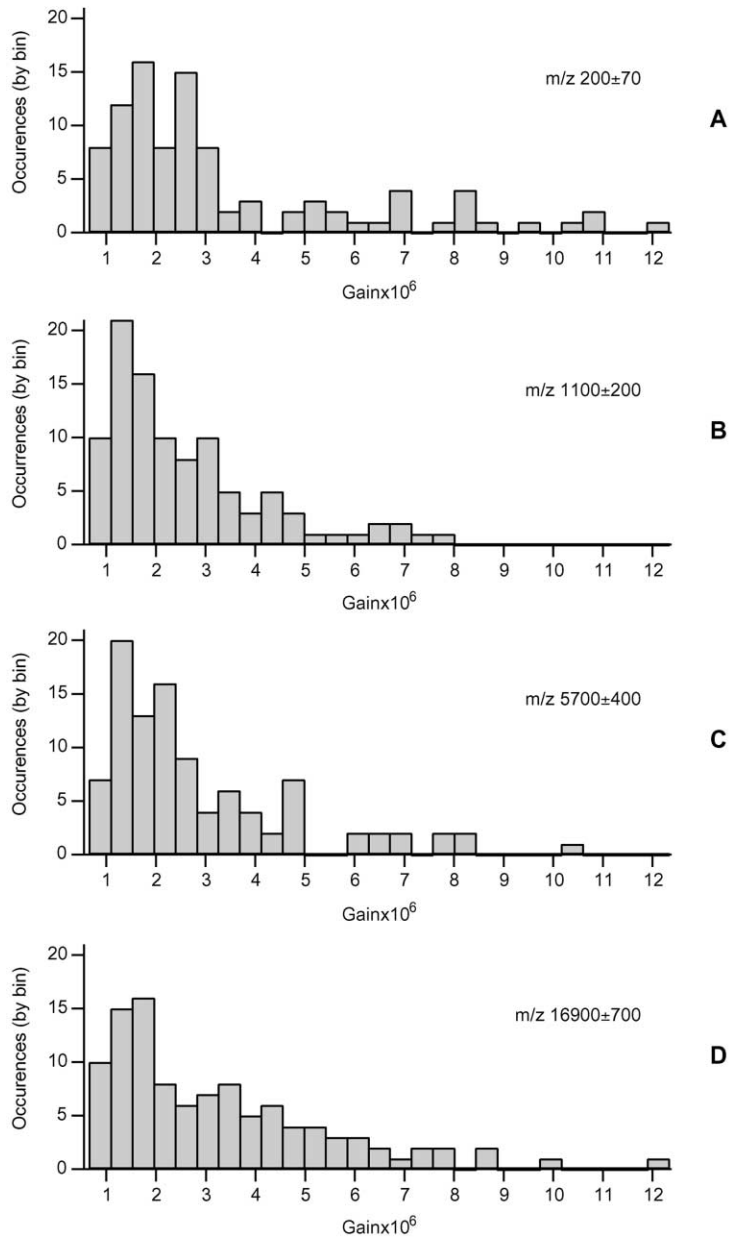

Fig. 5. Distribution of gains obtained for single ion peaks when detector bias was set to 3.15 kV. (A) Represents results for matrix ions, (B) for gramicidin S, (C) for insulin, and (D) for myoglobin, with the mass range listed on each plot.

Distributions for separate mass ranges are shown in each case.

Net gain was expected to decrease with mass because of decreasing numbers of initial secondary electrons. Such changes should not affect the location of the modes, unlike varying the bias. Thus, results for the different masses were pooled at each detector bias to make it easier to detect multimodal effects, since the larger number of data points should provide a smoother distribution. The resulting histograms are

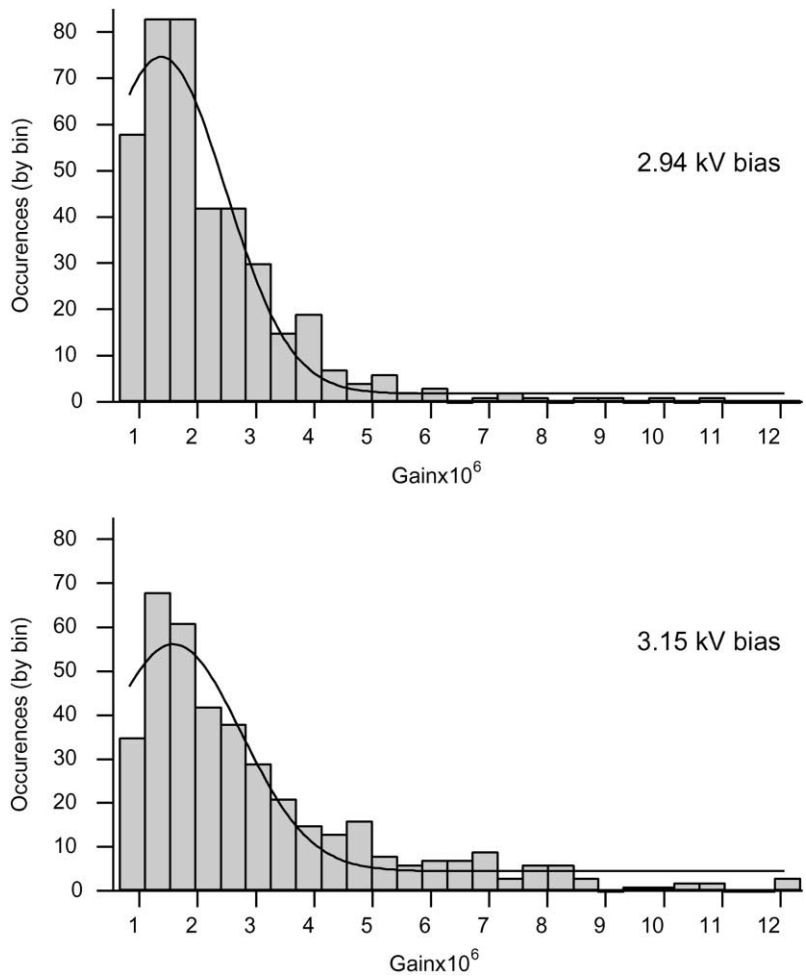

Fig. 6. Distribution of gains obtained for single ion pulses at the two detector bias settings, 2.94 and 3.15 kV. Results for different masses have been pooled and a Gaussian curve has been fitted to each histogram.

plotted as Fig. 6. A Gaussian fit is shown for the two plots in Fig. 6, to provide an indication of whether the data is normally distributed.

All histograms show a sharp low gain cut-off, modal values at a gain of 1×10^6 to 2.5×10^6 and a high gain tail. The sharp low gain cut-off was due to the instrument's limit of detection (three times *S*/*N*). There probably were smaller single ion signals, but these were classed as noise and not recorded or analysed. The modal value does not appear to shift much for the individual masses and there is no clear shift in the distribution to lower gain as mass increases. In fact, the distribution for the highest mass, given at (D) in the figures, shows more high gain results than those found for lower mass analytes (B and C), the opposite to what would be expected if high mass ions caused less initial secondary electron emission. This suggests that, regardless of mass, most ions do not cause the emission of many initial secondary electrons. Alternately, other effects, such as detector saturation from even one initial secondary electron, or hotspots on the surface of the MSP, are eliminating or swamping any effect due to initial secondary electrons.

The pooled results in Fig. 6 indicate that the mode did not change as bias potential was increased by 210 V. The 40% increase in mean single ion gain was due to the presence of a larger high-gain tail. This suggests that increasing the bias does not improve gain evenly over the whole of the detector. Instead, the increased bias creates more hotspots on the detector, where a higher gain is experienced. The majority of the detector continues to behave as before. Neither set of pooled results generates a multimodal distribution. The distributions are fairly smooth, without the presence of clear shoulders. This provides further evidence that single ion collisions with the front face of the detector result in the emission of a single (or zero) secondary electrons. Additionally, it appears that the detector response is not saturated by single initial secondary electrons, since response was able to increase with increasing bias.

This allows the detector performance to be explained in the following manner. Each ion incident upon the detector when standard operating potentials are applied causes the emission of (typically) zero or one initial secondary electron. If more than zero initial secondary electrons are emitted, the detector provides signal amplification of 1×10^6 to 3×10^6 for most ions, with amplification of up to 10^7 experienced at hotspots on the detector. Sensitivity decreases as mass increases, because at higher mass each ion incident on the detector has a lower probability of causing initial secondary electron emission. Hotspots on the detector are, however, slightly more efficient at detecting very high mass ions (such as myoglobin) than the rest of the detector when compared to low mass ion detection. Thus, although *total* signal detected decreases for high mass ions, since most go undetected, the *average single ion* signal actually increases.

4. Conclusion

The performance of a 70 mm microsphere plate detector was measured in a 20 kV oa-TOFMS mass spectrometer. The results indicate excellent temporal characteristics and high gains when ions generate secondary electrons on the surface of the detector. Close examination of single ion pulses reveals a relatively flat gain characteristic up to *m*/*z* 17,000, indicative of low secondary electron conversion efficiency in the current configuration. The tails of the frequency distributions of gains for ions of different *m*/*z* also suggests the presence of "hotspots" on the detector.

Acknowledgements

The continuing funding of the Australian Research Council is gratefully acknowledged. El-Mul Technologies (Yavne, Israel) are thanked for supplying an MSP plate for evaluation.

References

[1] J.N. Coles, M. Guilhaus, J. Am. Soc. Mass Spectrom. 5 (1994) 772.
[2] R.W. Nelson, D. Dogruel, P. Williams, Rapid Commun. Mass Spectrom. 9 (1995) 625.
[3] H. Wollnik, Mass Spectrom. Rev. 12 (1993) 89.
[4] M. Guilhaus, D. Selby, V. Mlynski, Mass Spectrom. Rev. 19 (2000) 65.
[5] R. Naaman, Z. Vager, Low-Vacuum Mass Spectrometer, Yeda Research and Development Co. Ltd., United States, 1999.
[6] A.S. Tremsin, J.F. Pearson, J.E. Lees, G.W. Fraser, Proc. SPIE 2518 (1995) 384.
[7] A.S. Tremsin, J.F. Pearson, J.E. Lees, G.W. Fraser, Nucl. Instr. Methods Phys. Res. A 368 (1996) 719.
[8] R. Naaman, Z. Vager, Rev. Sci. Instrum. 67 (1996) 3332.
[9] C. La Lau, in: A.L. Burlingame (Ed.), Advances in Analytical Chemistry and Instrumentation: Topics in Organic Mass Spectrometry, Mass Discrimination Caused by Electron-Multiplier Detectors, Vol. 8, Wiley, New York, 1970, p. 93.
[10] G. Westmacott, M. Frank, S.E. Labov, W.H. Benner, Rapid Commun. Mass Spectrom. 14 (2000) 1854.
[11] D.S. Selby, V. Mlynski, M. Guilhaus, Int. J. Mass Spectrom. 210/211 (2001) 89.
[12] B. Spengler, J. Mass Spectrom. 32 (1997) 1019.